CONF-8809173--1

UCRL--99582

DE89 001717

KINETIC SIMULATION OF MAGNETIC RECONNECTION IN THE PRESENCE OF SHEAR

Gregory E. Francis, Dennis W. Hewett, and Claire E. Max

Institute of Geophysics and Planetary Physics
Lawrence Livermore National Laboratory
University of California
Livermore, CA 94550

This paper was prepared for submittal to the
"International Workshop on Reconnection in Space Plasma"
Potsdam, East Germany, September 5-9, 1988

KINETIC SIMULATION OF MAGNETIC RECONNECTION IN THE PRESENCE OF SHEAR

Gregory E. Francis, Dennis W. Hewett, and Claire E. Max
Institute of Geophysics and Planetary Physics
Lawrence Livermore National Laboratory
University of California
Livermore, CA 94550

ABSTRACT

The basic physical processes associated with collisionless magnetic reconnection are investigated using the implicit PIC code AVANTI. The code is based on a 2.5-D fully electromagnetic direct implicit algorithm which has proven stable for arbitrary time step. This stability makes it possible to separate out the respective roles of the highly magnetized electrons and the un-magnetized ions for large ion-electron mass ratios. It is found that the inclusion of a guide magnetic field (magnetic shear) severely slows the initial stages of reconnection and damps out the electrostatic ringing if local values of the guide field are above a threshold determined by questions of electron mobility.

Keywords: Collisionless Reconnection, Implicit PIC Simulation, Electrostatic Effects, Magnetic Shear, Particle Jetting

1. INTRODUCTION

This paper is an extension of research recently published elsewhere by the authors,[1] and is a continuation to the work presented at this conference by Hewett, Francis, and Max[2] (hereafter referred to as Paper I).

In simplest form reconnection in a *collisional* plasma can be modeled using the MHD equations with a fixed value for the plasma resistivity. This yields a reduced, one-fluid description in which the large-scale topology and dynamics of reconnecting regions can be studied. By contrast, *collisionless* reconnection of magnetic field lines depends on electron inertia effects and the detailed behavior of the electron distribution function to provide the necessary freedom for magnetic topology changes. The formation of a non-Maxwellian tail on the ion distribution can be an important observed consequence of collisionless reconnection. Hence a faithful computational model must include a kinetic description of both electrons and ions.

Although traditional explicit particle-in-cell (PIC) techniques provide this description, stability requirements restrict simulation parameters to artificially small ion-to-electron mass ratios (e.g. $M_i/m_e \approx 10$ to 25), and short temporal periods (e.g. 100 plasma periods ω_{pe}^{-1} or less)[3]. In the present paper a new 2.5D fully electromagnetic Direct Implicit PIC plasma simulation code AVANTI[4] allows us to follow the dynamics of collisionless reconnection for all relevant M_i/m_e, and for a factor or 2 to 3 longer timescales. Details of this method can be found in Hewett and Langdon[4] and references therein. Since we are no longer constrained to resolve purely electromagnetic modes or ω_{pe} oscillations, we typically we use $\omega_{pe}\Delta t \approx 1$-2. Overall, we estimate that this implicit technique has expanded the parameter regime that can be studied by at least an order of magnitude. We have exploited this new advantage to simulate physically realistic mass ratios that reveal qualitatively new behavior.

2. LARGE M_i/m_e EFFECTS

The simulation parameters defining the initial equilibrium of our system have been described in detail in Paper I. For completeness, we here repeat the major features which define the equilibrium. Starting with a constant ion temperature and a Gaussian ion density profile we derive the initial equilibrium fields shown in Figure 1(a). The initial neutral sheet width δ is $2c/\omega_{pi}$. Larmor radii for electrons and ions outside of the neutral sheet are $\rho_e = 0.4c/\omega_{pi}$ and $\rho_i = 20c/\omega_{pi}$, respectively. This equilibrium resembles the Harris equilibrium,[5] but the ions carry no current, and are electrostatically confined. We also allow for anisotropy in electron temperatures parallel ($T_{e\parallel}$) and perpendicular ($T_{e\perp}$) to the initial magnetic field.

Figure 1(b-d) shows the time evolution of the magnetic field topology for a typical simulation. Contours of magnetic flux are shown as solid lines; the innermost (dotted) contour is the "separatrix", inside of which lies magnetic flux that has become trapped due to reconnection. Frame 1(b) shows the magnetic configuration characteristic of the early stages of reconnection, before the ions have had time to move. The electron current at the neutral sheet has already formed small-scale filaments, resulting in several magnetic X-points within the simulation volume. Later, Figure 1(c) shows that some of these small-scale filaments have coalesced. Still later, when enough time has passed for ion dynamics to become important, we see one remaining magnetic island, as in Figure 1(d).

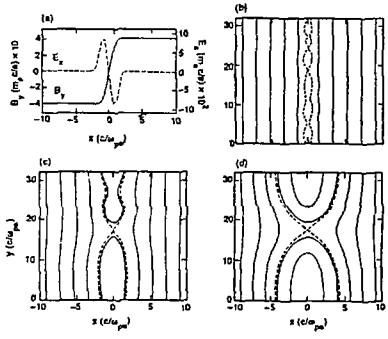

Figure 1. a) Profiles of initial electrostatic field E_z (dashed) and magnetic field B_y (solid) across the neutral sheet. Both fields have units of $m_e c\omega_{pi}/e$. The sheet current in the z direction is carried by electrons. Ions are contained by the electrostatic field. The initially uniform electron and ion temperatures are $T_{e\perp}/m_e c^2 = 2.8 \times 10^{-2}$, $T_{e\parallel} = (4/9)T_{e\perp}$, $T_i/m_e c^2 = 8.0 \times 10^{-2}$. (b-d): Magnetic flux contours (solid) and separatrix (dotted) in x-y plane: (b) At $t = 30\omega_{pi}^{-1}$, showing small-scale electron-driven filaments; (c) At $t = 160\omega_{pi}^{-1}$, as coalescence begins; (d) At $t = 410\omega_{pi}^{-1}$, with only one X-point remaining.

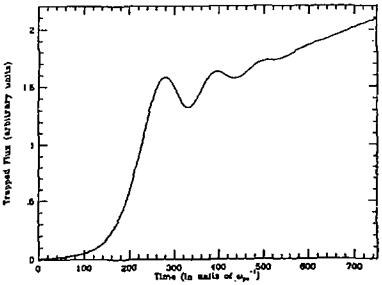

Figure 2. Trapped flux vs time for a representative simulation run. The electron and ion temperatures are as given in Fig. 1a, and $M_i/m_e = 2000$.

In Fig. 2 the several stages of spontaneous, collisionless reconnection are clearly isolated and distinguished. The early exponential growth of magnetic flux being trapped in the magnetic islands is consistent with predictions made by linear electron tearing mode theory,[6] providing consideration is made in the theory for the inclusion of the electrostatic effects.[7] This growth of the most unstable tearing mode in the simulation region dominates over the slower algebraic growth of the coalescence instability[8] as smaller islands form and then pair-wise coalesce. The end of this exponential growth occurs as the last two remaining islands are coalescing to form the one remaining O-point. For large ion-electron mass ratios ($M_i/m_e \geq 200$), this transition is accompanied by an electrostatic ringing, in which electron jetting into the surviving O-point builds up an ambipolar potential that in turn drives electrons back out of the magnetic island. The driving force of the ambipolar potential and the inertia of the jetting interact to produce an oscil-

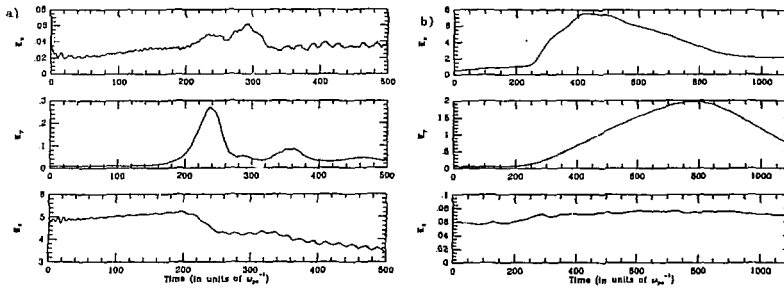

Figure 3. Directed kinetic energy of the: a) electrons as a function of time, indicating electron jetting only in the y-direction. The reduction of current-aligned (z-directed) energy coincident with the electron jetting is due to the presence of an inductive E_z in the region of the X-point, consistent with $\mathbf{E} \times \mathbf{B}$ driven jetting; b) ions as a function of time indicating ion jetting in first the x- and then the y-direction. This jetting is electrostatically driven by the ambipolar potential at the O-point.

lation of electrons and their associated magnetic flux into and out of the O-point. The electron jetting is evidenced in Fig. 3(a) as an increase in the y-directed kinetic energy of the electrons. Contour maps of electrostatic potential show that the jetting electrons are leaving the X-point region to flow into the O-point. Note that the two apparent incidences of jetting are accompanied by decreases in the current-aligned (z-directed) energy. This is due to the generation of an inductive normal component of electric field E_z, consistent with an $\mathbf{E} \times \mathbf{B}$ driving mechanism. This electrostatic ringing is seen in Fig. 2 to be superimposed on a constant linear growth of trapped flux into the island. This late-time, ion-mediated reconnection swells the remaining magnetic island as ions and electrons enter together through the X-point at the ion acoustic speed, $v_s = \sqrt{T_e/M_i}$. This region was studied in detail in Paper I. The migration of bulk plasma into the island is seen as ion jetting in Fig. 3(b).

3. MAGNETIC SHEAR

The addition of a zeroth-order magnetic field aligned with the sheet current retains most of the features of the simulations just described. We report here the findings of an on-going parametric study of the effects of magnetic shear on the reconnection process. The magnetic shear is introduced through the inclusion of a zero order dc magnetic field in the z-direction which is initially taken to be uniform across the simulation plane. We began this study in an attempt to connect our previous findings without shear to problems in laboratory plasmas, such as tokamaks, compact toroids, reversed-field pinches, and the reconnection experiments of Stenzel and Gekelman.[9] In these systems magnetic reconnection takes place in the presence of magnetic shear.

In Fig. 4 we plot the time histories of trapped flux for four different values of the initial guide magnetic field B_{z0}. The first thing to be noted from Fig. 4 is that much of the basic physics involved in collisionless magnetic reconnection appears to be unaffected by the inclusion of a guide magnetic field. Of note are two exceptions to this observation. First, there appears to be a discontinuous, or at least non-linear, decrease in the initial growth rate between the simulation runs having $B_{z0} \simeq B_0 \equiv 0.12$ and $B_{z0} = 2B_0$. This can be understood by looking at the threshold for B_{z0}, above which the electrons in the neutral sheet are no longer un-magnetized. We define this threshold B_{zc} such that the electron Larmor radius in the neutral sheet $\rho_e(x = 0)$ is equal to the geometric mean of the neutral sheet width δ and the electron Larmor radius outside of the neutral sheet $\rho_e(x >> \delta)$:

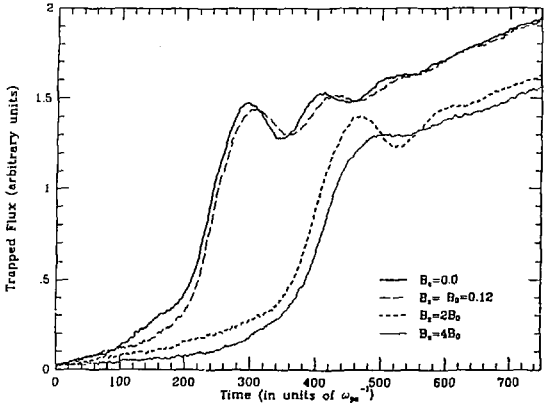

Figure 4. Trapped magnetic flux vs time for four different values of the initial guide magnetic field B_{x0}. Electrons in the neutral sheet are strongly magnetized for $B_{x0} \geq 0.18$.

$$\rho_e(z=0) = \sqrt{\delta \rho_e(z >> \delta)}, \quad \text{for } B_{x0} \approx B_{xc}. \qquad (1)$$

This calculation yields a critical guide field of $B_{xc} = 0.18$, above which the neutral sheet electrons are magnetized and no longer free to stream. Note that this critical value of B_{x0} lies halfway between that of the two runs in question.

The second point to make from Fig. 4 is that the electrostatic ringing is apparently unaffected by the transition above B_{xc}: the amplitude of the oscillation of electrons and magnetic flux into and out of the magnetic island is just as large for the case $B_{x0} = 2B_0 > B_{xc}$ as it is for $B_{x0} = B_0 < B_{xc}$. It is not until B_{x0} is raised to $4B_0$ ($>> B_{xc}$) that the electrostatic ringing is damped away by the increased viscosity in the system. Since the ringing is a manifestation of electron jetting (free streaming into

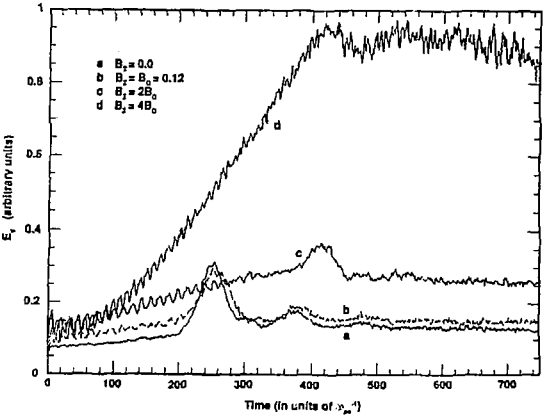

Figure 5. Time histories of the y-directed energy of the electron component for the four values of B_{x0} in Fig. 4.

the O-point), we would not expect to see the ringing above B_{xc}. Indeed, Fig. 5 verifies that electron jetting still exists for the $B_{x0} = 2B_0$ case, but that the electrons are too strongly magnetized to jet in the $B_{x0} = 4B_0$ case. To explain this apparent discrepancy, we look at a contour map of guide magnetic field for the case $B_{x0} = 2B_0$ (see Fig. 6a). We find that as electrons are gathered and heated inside of a magnetic island, the B_z in the island is reduced from its initial uniform value B_{z0}. This "hollowing out" of the guide magnetic field at an island is perhaps due to the increased diamagnetic field contribution of the bunched, hot electrons in the O-point. Figure 6(a) shows that at the time $t = 410\omega_{pi}^{-1}$, when the $B_{x0} = 2B_0$ case is making the transition between the exponential growth of the electron tearing mode and the linear growth of the ion-mediated reconnection, the guide field in the magnetic island has been reduced through this hollowing-out process to values below the threshold B_{zc}, thus allowing the neutral sheet electrons to jet. A similar map for the case $B_{x0} = 4B_0$ shows that the guide field is not reduced below the threshold at the time of transition, hence the electrostatic ringing is damped.

4. DISCUSSION

Magnetic reconnection simulations without the sheared magnetic field[1,2] reviewed here provide a good foundation for the new simulations reported in this paper. Generally, the sheared magnetic field configuration displays much of the behavior observed in the nonsheared studies. In particular, spontaneous reconnection can occur in both cases, it can be characterized as having three regimes, and with small enough B_{z0}, can exhibit the late time oscillation of the trapped flux mediated by the ion mass.

In some cases, however, the plasma is unable to mimic zero-shear behavior until it has expelled enough B_z so that local values are below thresholds determined by questions of electron mobility. We find, in particular, that the rapid coalescence of small filaments into large current channels at the O-points are inhibited until the B_z field along the original B_y field null is suitably reduced. Similarly, the zero-shear simulations exhibited flux oscillations as the unmagnetized electrons respond to $\mathbf{E} \times \mathbf{B}$ and ambipolar forces. We find that with strong shear this oscillation is inhibited unless the local field is below a threshold B_{zc}.

This research was performed under the auspices of the U.S. Department of Energy by the Lawrence Livermore National Laboratory under contract no. W-7405-ENG-48.

References

[1] D.W. Hewett, G.E. Francis, and C.E. Max, "New Regimes of Magnetic Reconnection in Collisionless Plasmas", Phys. Rev. Lett. 61, 893, August 15, (1988).

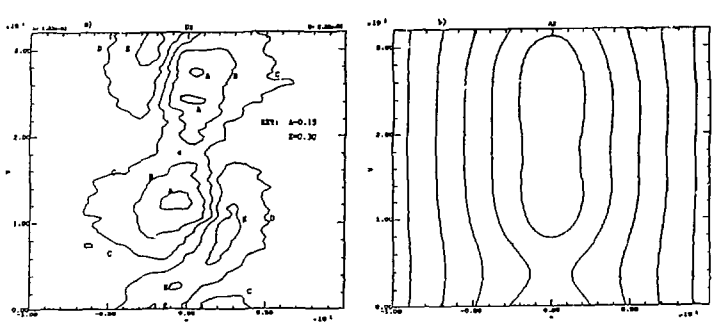

Figure 6. a) Contour map of the guide magnetic field at time $t = 410\omega_{pi}^{-1}$ for the case $B_{x0} = 2B_0 = 0.24$ of Fig. 4. The field inside of the island is below the threshold B_{zc}. b) Magnetic flux contours at the same time indicating the position of the magnetic island.

[2] D.W. Hewett, G.E. Francis, and C.E. Max, "Magnetic Reconnection Simulation Using the 2.5-D EM Direct Implicit Code AVANTI", at this conference.

[3] J.N. Leboeuf, T. Tajima, and J.M. Dawson, Phys. Fluids **25**, 784 (1982); J.N. Leboeuf et al., in *Magnetic Reconnection in Space and Laboratory Plasmas*, edited by E.W. Hones (Am. Geophys. Union, Washington DC, 1984), pg. 282; M. Hoshino, J. Geophys. Res. **92**, 7368 (1987).

[4] D.W. Hewett and A.B. Langdon, J. Comp. Phys. **72**, 121 (1987).

[5] E.G. Harris, Nuovo Cimento **23**, 115 (1962).

[6] G. Laval, R. Pellat, and M. Vuillemin, in *Plasma Physics and Controlled Nuclear Fusion Research* volume 2 (I.A.E.A., Vienna, 1966), page 259; See also summary in Hones (ref. 3), pages 311-315.

[7] I. Katanuma and T. Kamimura, Phys. Fluids **23**, 2506 (1980); M. Hoshino, op. cit.

[8] A. Bhattacharjee, F. Brunel, and T. Tajima, Phys. Fluids **26**, 3332 (1983).

[9] R.L. Stenzel and W. Gekelman, J. Geophys. Res. **86**, 649 (1981); W. Gekelman and R.L. Stenzel, J. Geophys. Res. **86**, 659 (1981).